SUPERSATURATION OF IRON WITH NITROGEN, HYDROGEN OR CARBON AND THE CONSEQUENCES

PRENASIČENJE ŽELEZA Z DUŠIKOM, VODIKOM ALI OGLJIKOM IN POSLEDICE

Hans Jürgen Grabke

Max-Planck-Institut für Eisenforschung GmbH, Abt Physikaliche chemie, 40074 Düsseldorf, Germany
grabke@mpie.de

Reactions leading to supersaturation of iron with nitrogen, hydrogen or carbon are described and some of the consequences of the supersaturation. The formation of the thermodynamically stable state of the elements, N_2(gas), H_2(gas) and graphite from the supersaturated solid solutions may cause defects or even destruction of iron and steels. High nitrogen concentrations and instable nitrides are attained in flowing NH_3-H_2 mixtures, in a steady state where nitrogenation is fast but N_2-desorption slow, the supersaturation leads to porosity by N_2-formation in the metal or in the nitride layer. High hydrogen concentrations are established by the electrochemical reactions in pickling or by annealing at elevated temperatures, and may cause porosity in steels or blistering of coatings by H_2-formation. Supersaturation with carbon occurs in nonequilibrium gas atmospheres, e.g. syngas CO-H_2 and leads to disintegration of iron and steels by graphite formation, after cementite has formed as an intermediate. Parallels and similarities in these processes are pointed out.

Keywords: iron, steel, supersaturation, steady state, porosity, blistering, metal dusting

Opisane so reakcije, ki vodijo do prenasičenja železa z dušikom, vodikom, ogljikom, in nekatere posledice. Formiranje termodinamično stabilnega stanja elementov: N_2(plin), H_2(plin) in grafit, iz prenasičene trdne raztopine lahko povzroči poškodbe ali celo propad železa in jekla. Visoka koncentracija dušika in nestabilni nitridi, izpostavljeni plinski mešanici NH_3-H_2, v stabilnem stanju, kjer je nadušičenje hitro, toda desorpcija dušika počasna, prenasičenje vodi do poroznosti zaradi formiranja N_2 v kovinah ali v nitridni plasti. Visoka koncentracija vodika nastaja v elektrokemijskih reakcijah pri luženju ali pri žarjenju pri povišanih temperaturah, povzroča poroznost v jeklih oziroma tvorbo mehurčkov H_2 v prevlekah. Prenasičenje z ogljikom nastaja v neravnovesnih plinskih atmosferah, kot npr. v plinu CO-H_2,in vodi do tvorbe grafita, potem ko se je najprej oblikoval cementit, in tako do razkroja železa in jekel. Prikazane so vzporednosti in podobnosti med opisanimi procesi.

Ključne besede: železo, jeklo, prenasičenje, stabilno stanje, poroznost, tvorba mehurčkov, kovinsko oprašenje

1 INTRODUCTION

Most important for the properties of iron and steels are the contents of the nonmetals carbon, nitrogen and hydrogen. Very useful effects can be exerted by C and N, concerning mechanical strength, hardness, wear and corrosion resistance, whereas H may cause a lot of trouble by flaking, blistering, cracking and embrittlement of steels. An immense knowledge and a vast literature exist on the important systems Fe-C, Fe-N and Fe-H, and it may be noted that some aspects were covered in earlier reviews in this journal: "Absorption and Diffusion of Hydrogen in Steels" [1] and "Carburization, Carbide Formation, Metal Dusting, Coking" in and on iron and steels [2]. Supersaturation is obtained often and easily in different ways in these systems, and sometimes leads to useful properties of the materials, but also can cause defects and destruction, since in the supersaturated solutions the strong tendency exists for formation of the thermodynamically stable states of the elements, of graphitic carbon resp. of the diatomic gases N_2 or H_2. As yet, the processes and reactions leading to supersaturation and the formation of the stable state have not been considered under common terms for the systems Fe-C, Fe-N and Fe-H, so this paper is meant to demonstrate some parallels in the formation and decomposition of supersaturated states in these systems.

2 SUPERSATURATION AND PORE FORMATION IN THE SYSTEM Fe-N

Nitrogen can be dissolved in iron according to the reaction

$$N_2 = 2 \text{ [N]} \tag{1}$$

where [N] stands for dissolved nitrogen atoms. According to the mass action law for the dissolution of diatomic gases in metals, which is known as Sieverts' law, the concentration is proportional to the square root of the pressure

$$c_N = K_1 \cdot (p_{N_2})^{1/2}$$

The solubility in equilibrium with N_2 at 1 bar is very low, in α-iron the solubility is increasing with temperature to about 40 µg/g at 900 °C and in γ-iron the solubility is nearly temperature independent, about the mass fraction 0.025 %, see **Table 1** [3]. At all higher concentrations, the iron is supersaturated, and also all iron nitrides: γ'-Fe$_4$N, ε-Fe$_{2-3}$N and ζ-Fe$_2$N, see phase diagram **Figure 1a** [4], are thermodynamically instable

and nitrogen desorption should occur from the super-saturated iron or the iron nitrides. The reaction (1) plays no great role in practice, since the dissociation of molecular nitrogen needs a high activation energy and is very sluggish at temperatures below 1000 °C, only in steel corrosion at higher temperatures nitridation by N_2 (from air or protective atmospheres) plays a role [5]. On the other hand, N_2-dissociation must take place for NH_3-synthesis, and actually iron catalysts with special orientation and high surface area are used in this important industrial process.

Table 1: Solubility of nitrogen in iron ($\mu g/g$) [2]
Tabela 1: Topnost dušika v železu (masni deleži $w/(\mu g/g)$) [2]

$T/°C$	At 1bar N_2	At equil. α-Fe/F$_4$N	p_{N_2} (bar)
20	$4.1 \cdot 10^{-3}$	0.079	362
100	0.059	1.7	814
200	0.46	18	1524
300	1.7	84	2294
400	4.5	250	3057
500	9.0	550	3782
590	15	970	4382
700	24		
800	33		
910 (γ)	266		
1400 (γ)	206		
1400 (δ)	112		
1540 (δ)	132		
1540 (liq.)	444		

The phases with high nitrogen content are easily prepared by nitriding in flowing NH_3-H_2 mixtures at 1 bar, according to the reaction

$$NH_3 = [N] + 3/2\ H_2 \qquad (2)$$

where [N] stands for dissolved nitrogen or N in a nitride. Already in 1930 Lehrer [6] published the well-known diagram, showing the ranges of phase stabilities for α, γ, γ' and ε in dependence on temperature and NH_3 content of the atmosphere, see **Figure 1b** for reaction (2). From the mass action law the "nitriding potential" (Nitrierkennzahl) of the NH_3-H_2 mixture results

$$r_N = \frac{p_{NH_3}}{(p_{H_2})^{3/2}}$$

which is used to characterize the nitriding activity of a medium used for nitriding of steels, to harden the surface [7,8]. By considering the ammonia decomposition and formation reaction

$$2\ NH_3 = N_2 + 3\ H_2, \quad p_{N_2} = K_3 \frac{(p_{NH_3})^2}{(p_{H_2})^3} = K_3 \cdot r_N^2 \qquad (3)$$
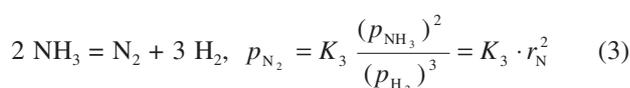
the nitriding potential can be related to the equilibrium nitrogen pressure of the NH_3-H_2 gas mixtures. From calculation of this nitrogen pressure with data for the
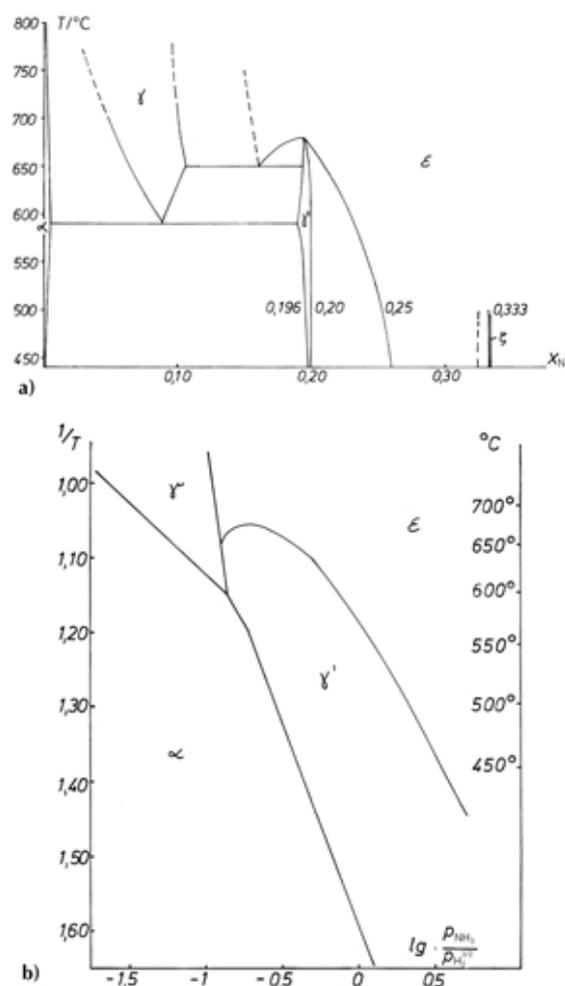
Figure 1: Phase diagram of the binary system Fe-N, (a) in a plot temperature versus mole fraction [3,4] and (b) in a plot (Lehrer-diagram) of temperature versus nitriding potential [6]
Slika 1: Fazni diagram binarnega sistema Fe-N, a) v grafičnem prikazu temperatura proti molskemu deležu [3,4] in b) v grafičnem prikazu (Lehrerjev diagram) temperatura proti potencialu nadušičenja [6]

ammonia synthesis (Fritz Haber and other work) enormous values result, which can only be virtual pressures, e.g. at $r_N = 0.1$

550 °C: $1.9 \cdot 10^3$ bar N_2,
700 °C: $1.8 \cdot 10^4$ bar N_2,
950 °C: $2.3 \cdot 10^5$ bar N_2.

These thermodynamic considerations indicate the strong tendency for nitrogen desorption from the super-saturated phases:

$$2\ [N] \rightarrow N_2$$

However, this reaction and also its forward reaction (1) have high activation energies and are very slow at the usual nitriding and nitrocarburizing temperatures 500–600 °C. The kinetics of reaction (1) and (2) have been studied, using resistance-relaxation measurements on thin iron foils [9]. Rate equations have been obtained and the steady-state situation was described, see **Figure 2**, which establishes the nitrogen content of an iron
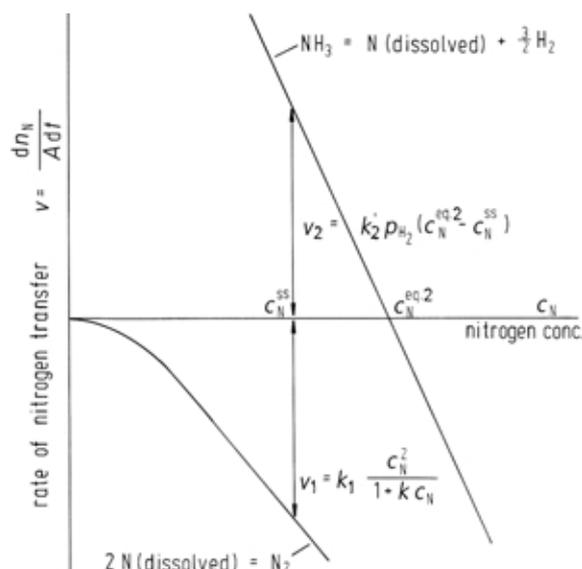
Figure 2: Steady state in the nitrogenation of iron in a flowing NH_3-H_2 mixture, established at the steady state concentration c_N^{ss} where the rate of N-transfer from NH_3, reaction (2) is equal to the rate of N_2 desorption, more or less below the equilibrium for reaction (2) at $c_N^{eq.2}$, schematics and rate equations [9]

Slika 2: Stabilno stanje pri nadušičenju železa v plinski mešanici NH_3-H_2, ugotovljeni pri stabilni koncentraciji c_N^{ss}, kjer je stopnja prenosa N iz NH_3 reakcija (2), enaka stopnji desorpcije N_2, več ali manj pod ravnovesjem za reakcijo (2) pri $c_N^{eq.2}$, shematične in ravnovesne enačbe [9]

Figure 3: Change of nitrogen content W_{N_2} in iron foils (cold rolled or annealed), treated in an H_2-0.97 % NH_3 atmosphere at 950 °C, – fast nitrogenation and after void formation start of slow denitrogenation by N_2-desorption, – fast denitrogenation in the carburizing atmosphere without NH_3 [10]

Slika 3: Sprememba vsebnosti dušika v folijah Fe (hladno valjane ali žarjene), obdelane v plinski atmosferi H_2-0,97 % NH_3 pri 950 °C – hitro nadušičenje in po tvorbi praznin počasno razdušičenje z N_2-desorpcijo – hitro razadušičenje v naogljičevalni atmosferi brez NH_3 [10]

sample in a flowing NH_3 – H_2 mixture. The steady state concentration c_N^{ss} results, where the rate of nitrogen transfer from NH_3 – H_2 is equal to the rate of nitrogen desorption, and since at low temperature < 600 °C generally $k_1 \ll k_2$, the steady state concentration is only negligibly smaller than $c_N^{eq.2}$, the equilibrium concentration for reaction (2). For higher temperatures, however, the difference increases markedly. Therefore it becomes dubious, to base thermodynamic considerations and derivations on the equilibrium of reaction (2) at elevated temperatures, as done in some studies on the iron nitrides.

The high virtual nitrogen pressures in supersaturated iron and in the iron nitrides and the tendency to formation of molecular nitrogen can lead to **porosity**, i.e. formation of pores containing gaseous nitrogen. This void formation was observed during nitrogenation of iron foils and steel in the austenitic region [10,11]. Samples were analyzed for their nitrogen content and presence of voids after nitriding runs in atmospheres with 0.08 – 1.59 % NH_3 and appearance of voids was detected at the mass fractions of nitrogen contents > 0.6 % [10]. Related to the solubility of N in γ-iron, this means that the voids are formed at pressures p_{N_2} > 400 bar. Nucleation of the voids is occurring mainly at grain boundaries and inclusions of the steel. After some time, about 1 h at 850 °C the nitrogen content begins to decrease, see **Figure 3**, obviously because the pores have joined to channels and the nitrogen gas can leave the materials.

One may wonder, why the recombination of two nitrogen atoms, the N_2 formation does not take place already on the outer surface, but is possible in the iron on the walls of the voids and pores. However, studies of reactions (1) and (2) in the presence of H_2S or H_2O have shown, that reaction (1), the dissociation and recombination of nitrogen is strongly poisoned by adsorbed sulfur and/or oxygen [12-14] whereas reaction (2) is affected much less. Adsorbed S, O and other impurities will be present on steel surfaces in nitriding and carbonitriding atmospheres, while the walls of pores growing in the iron or steel will be clean, at least initially.

The formation of pores and later on channels in austenitic iron was clearly demonstrated also in a study by E. J. Mittemeijer et al. [11] on nitrogenation of iron at 700 °C – 810 °C in NH_3-H_2 mixtures. Austenitic regions are advancing from the outer surface and pores are formed at the austenite grain boundaries which develop on continued nitrogenation and are approximately perpendicular to the surface. After prolonged nitrogenation the pores coalesce and form channels in contact with the surface, see **Figure 4**. Thus the denitrogenation reaction (1) backwards can occur within the austenite, compensating the nitrogenation reaction (2) at the surface and finally leading to complete denitrogenation.

The preceding paragraphs concerned nitrogen in the γ-phase, but many studies have been conducted in flowing NH_3-H_2 mixtures, also on thermodynamics, disorder equilibria, kinetics of formation and diffusion of
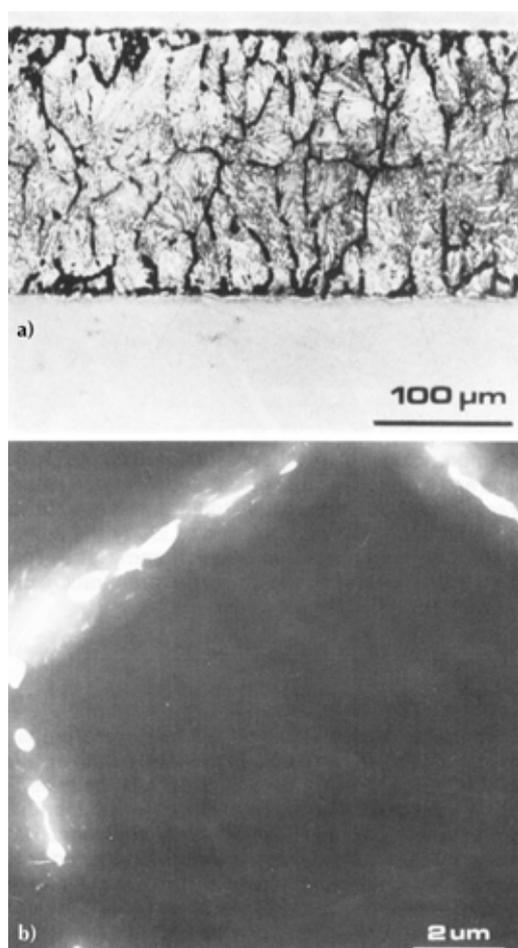
Figure 4: Pore and channel formation in austenite after nitrogenation of iron at 700 °C in H_2-9 % NH_3 for 3.5 h [11]; (a) optical micrograph of a metallographic cross section, (b) TEM micrograph, pores at grain boundaries

Slika 4: Tvorba por in kanalov v avstenitu po nadušičenju 3,5 h pri 700 °C in H_2-9 % NH_3 [11] a) svetlobna mikroskopija metalografskega vzorca, b) TEM-posnetek prikazuje pore na mejah zrn.

Figure 5: Evolution of the "compound layer" of γ'- and ε-nitride, during nitriding at 570 °C in 56 % NH_3-44 % H_2 [17]; (a) after 15 min ε/γ'-nuclei at the surface, (b) after 35 min ε/γ'-double layer, (c) after 8 h porosity in the ε-layer, predominantly at grain boundaries, but also in specific planes

Slika 5: Razvoj "zlitinske plasti" γ'- in ε-nitrida med nitriranjem pri 570 °C v 56-odstotni NH_3 – 44-odstotni H_2 [17]; a) po 15 minutah ε/γ'-nukleacije na površini b) po 35 min ε/γ'-dvojna plast c) po 8 h poroznost v ε-plasti, predominantno na mejah zrn kot tudi na specifičnih ploskvah

nitrogen in the γ'- and ε-nitride phases [15-19]. Their growth is important also in the technical nitriding and carbonitriding process, conducted on steel parts for hardening and improved wear resistance and corrosion resistance [7,8]. This process is performed at temperatures 500–590 °C in NH_3-H_2 or NH_3-H_2-CO-CO_2-H_2O (Endogas) mixtures. The so-called "compound layer" on iron and steels (**Figure 5**) grows by a) initial ingress of [N] in the α-phase, local nucleation of γ'-nitride which grows by nitrogen diffusion from the α-phase and through the nitride, b) nucleation of ε-nitride on the γ'-nitride and formation of the ε/γ'-double layer, further growing only by nitrogen diffusion through the nitrides. Then void nucleation and pore growth starts, c) at first at grain boundaries of the ε-nitride, later on d) also in the surface zone of the ε-phase and the pores at the grain boundaries join. Now denitrogenation by N_2 – desorption is beginning. In the case of nitrocarburising, carbon gets in

mainly by CO diffusion into the channels and C transfer into the ε-phase. In the fundamental studies, the pore formation generally was avoided, but in the technical process porosity certainly occurs, due to the high virtual pN_2 in the nitride layers. Many years even up to 1996 there was uncertainty in the heat treatment industry about the origin of the porosity [20-22], but surplus studies on the content and shape of the pores have confirmed that they in fact are "N_2 bubbles" (unpublished studies at the Max-Planck-Institut für Eisenforschung, 1986 and 1992).

The **porosity of the compound layer** certainly has negative effects on its mechanical stability and adherence, but due to its origin from the fundamental thermodynamic conditions of the process this effect cannot be avoided [21].

A special case of supersaturation with N was observed recently [23-25] upon low temperature nitriding of stainless steels, especially by nitrogen implantation, but also in a case of corrosion in a NH_3-CO_2 atmosphere [26]. Implantation of the stainless steels 304 and 310 at about 380–425 °C with N_2^+ was shown to produce a high N phase with $x_N = 20$–30 % N. This "γ_N" phase is charac-

terized by high hardness HV up to 1500 and therefore may be of interest for wear protection. Its lattice is an expanded austenite, with up to 26% volume expansion in relation to SS 304, which causes cracking and spalling of "γ_N" layers in the case of continued corrosion [26]. The nitrogen in this phase obviously is tied to the Cr atoms in the steel, and at temperatures higher than about 425 °C this γ_N-phase converts to bcc iron with CrN precipitates. A similar very hard phase with high carbon content was observed after "colossal carburization" of austenitic steels [27].

3 SUPERSATURATION AND BLISTERING IN THE SYSTEM Fe-H

Supersaturation with hydrogen can cause a lot of problems concerning the material properties of steels [28-38]. These effects can be due to formation of molecular hydrogen in voids, pores or at interfaces: porosity in castings and welds, "flaking" in large forgings, "exfoliation" of gas carburized specimens, "fisheyes", hydrogen induced cracking (HIC), formation of blisters after tin or zinc plating or after enamelling. But presence of hydrogen in a steel also can embrittle steels, just by H diffusion to a defect or a crack tip, leading to loss of coherence and enhanced crack propagation rates. Here the high diffusion velocity of H in ferritic steels [1,31] plays a great role, since even at ambient temperature and small hydrogen concentration the H atoms rapidly assemble and become adsorbed at the crack flanks and in the crack tip. These effects of atomic H need stress, and are known as hydrogen stress cracking (HSC) and hydrogen induced stress corrosion cracking (HISCC).

Considering all these problems it is clear that research and literature on hydrogen in iron and steels are immense, therefore here only some aspects will be discussed on the mechanisms leading to supersaturation, illustrated with some details from a recent study on the role of hydrogen in the production of galvanized hot-rolled steel strip [37,38]. In contrast to nitrogenation, the absorption of hydrogen from H_2 containing atmospheres plays an important role, since the reaction

$$H_2 = 2 \, [H] \tag{4}$$

can take place, forward and backward, rapidly even at rather low temperatures. The solubility of hydrogen in iron in equilibrium with H_2 at 1 bar is endothermic, and increasing with temperature, in α-iron from very low values and in γ-iron at a somewhat higher level, and the solubility in iron melts is considerably higher than in solid iron, see **Table 2** [3]. Accordingly, problems can arise upon solidification of iron melts, by porosity in the castings, and upon rapid cooling after welding, by weld cold cracking.

During annealing in H_2-containing gases, steel absorbs hydrogen easily and the equilibrium (4) is

Table 2: Solubility of hydrogen in iron at 1 bar H_2 [2]
Tabela 2: Topnost vodika v železu pri 1 bar H_2 [2]

T/°C	µg/g	$x_N \cdot 10^{-6}$	$cm^3 \, H_2$/ 100 g Fe
20	$5.4 \cdot 10^{-4}$	0.03	$6 \cdot 10^{-4}$
300	0.14	7.8	0.16
500	0.65	36	0.72
700	1.6	89	1.8
900 (α)	2.8	160	3.1
900 (γ)	4.2	230	4.7
1000	5.0	280	5.6
1200	6.8	380	7.5
1400 (γ)	8.4	470	9.3
1400 (δ)	6.7	370	9.4
1540 (δ)	7.7	430	8.6
23	23	1300	25

usually established, the hydrogen content being determined by Sieverts' law.

$$c_H = K_4 \cdot \sqrt{p_{H_2}}$$

This expectation was confirmed recently [37,38] by annealing hot rolled strip samples of two different steels (an Al-killed, unalloyed ELC steel with very low carbon content 0.03 % C, and a high strength dual phase steel DP 600) in N_2-20 % H_2, N_2-60 % H_2, N_2-80 % H_2 and pure H_2 at (500, 600 or 700) °C for (10, 20 or 30) min. The final H-content corresponded to the equilibrium content for the various temperatures and hydrogen pressures. (The data for the hydrogen content are even a bit lower than the literature values, – the reason is not quite clear, either these old values are not reliable, or there were some hydrogen losses before analysis in the present studies.) In the production process these steels are pickled, exposed to continuous annealing at 600 °C for 25 s and then coated in a galvanizing bath with zinc (Zn + 0.21 % Al or Zn + 0.21 % Al + 0.05 % Pb). Problems with **blistering** of the coating were observed, obviously due to the hydrogen absorption during annealing, since the extent of blistering clearly increased with the p_{H_2} of the annealing atmosphere.

In the pickling process, before continuous annealing, high H-contents are established in the steels, but this excess hydrogen is rapidly desorbed during the annealing. The hydrogen absorption during pickling or during any corrosion in acid environments is an important source of hydrogen in steels. The corrosion is an electrochemical process [39], mainly composed of the anodic dissolution of iron:

$$Fe = Fe^{2+} + 2e^- \tag{5}$$

and of the cathodic hydrogen formation:

$$2H^+ + 2e^- = 2H \text{ (adsorbed)} \quad \text{Volmer reaction} \tag{6}$$

$$2H \text{ (adsorbed)} = H_2 \text{ (gas)} \quad \text{Tafel reaction} \tag{7}$$
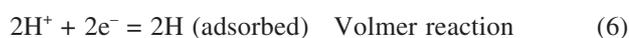
Beside these reactions also the electrochemical recombination can play a role:

H (adsorbed) + H$^+$ + e$^-$ = H$_2$ (gas)

Heyrovsky reaction   (8)
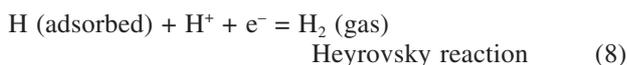
A steady state is established (similarly as in the case of nitrogenation by NH$_3$), mainly by the Fe dissolution reaction and the Volmer reaction. At equal currents of electrons resulting from the anodic dissolution and electrons used for discharging the H$^+$ ions from the electrolyte a steady state electric potential is fixed on the solid iron surface (see **Figure 6**) and a steady state coverage with adsorbed hydrogen. The adsorbed hydrogen will be absorbed also into the iron and one can usually assume an absorption equilibrium

H (adsorbed) = H (absorbed)   (9)
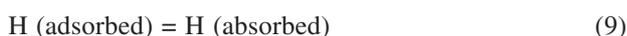
which is dependent on the interplay of the electrochemical reactions given above and dependent on the steady state potential. Presence of so-called "promoters" [40] such as H$_2$S and the hydrides of Se, Te, P, As, Bi and rhodanides or cyanides inhibits the recombination of the adsorbed H-atoms (Tafel reaction) and thus promotes the absorption of H into the metal. In this way, very high hydrogen activities can be established on corroding iron and steel surfaces and considerable amounts of H are absorbed. Measurement of the hydrogen activity on a corroding surface of an iron or steel membrane is possible by the permeation method, i.e. the determination of the steady state diffusion of H through the membrane in an electrochemical double cell [41,42]. Such studies have been conducted at the Max-Planck-Institut für Eisenforschung to a large extent, to find out about
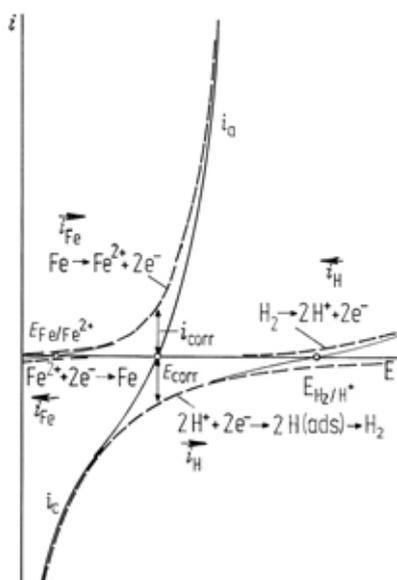
Figure 6: Steady state in the acid corrosion of iron, established at the corrosion potential E_{corr} where the anodic current of Fe-dissolution is equal to the cathodic current for the discharge of H$^+$ [39], leading to more or less H-absorption in iron when the H$_2$-desorption (Tafel reaction) is poisoned.

Slika 6: Stabilno stanje med kislinsko korozijo železa, dokazan pri korozijskemu potencialu E_{corr} kjer je anodni tok Fe-razkroja enak katodnemu toku za izločanje H$^+$ [39], ki vodi več ali manj do H-absorpcije železa , ko je H$_2$-desorpcija (Tafel-reakcija) izmaličena
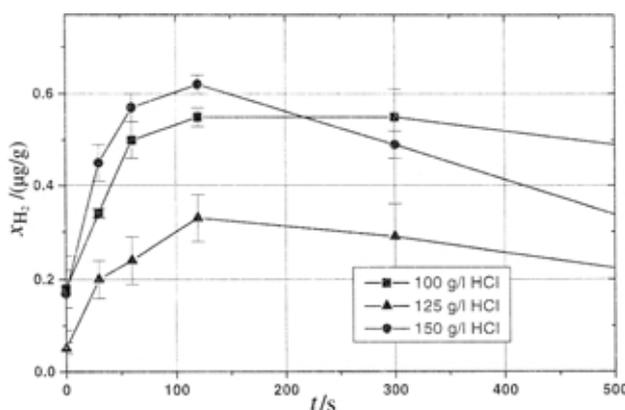
Figure 7: Hydrogen determinations in the low carbon steel after pickling in HCl at different concentrations, in dependence on pickling time, demonstrating H$_2$-desorption after continued pickling, in practice pickling is conducted for only 10 s [37,38].
Slika 7: Slika 7 Določitev vodika v nizkoogljičnih jeklih po luženju v HCl raličnih koncentracij v odvisnosti od časa luženja prikazuje H$_2$-desorpcijo po nadaljevanju luženja; v praksi se luži samo 10 s [37,38].

effects of alloying elements on the corrosion and H absorption of iron [34-35] but also on effects of inclusions, precipitates and microstructure on the hydrogen diffusion, solubility and trapping in steels [46-50].

But now back to the study on "Galvanising of Hot-Rolled Steel Strip" [37,38] in which also the hydrogen absorption upon pickling in HCl was investigated. In the different steels a steady state hydrogen content was attained after about 100–200 s, of about 0.5–2 μg/g hydrogen, depending on pickling conditions and type of steel, see **Figure 7**. Considering the equilibrium solubility (**Table 2**), these data correspond to an enormous supersaturation. One must assume that the major part of this hydrogen is not present in the normal iron lattice, but absorbed in "traps", i. e. sites with more space and higher binding energy for the H-atoms, such as grain boundaries, dislocations, interfaces of inclusions and precipitates and even mesoscopic defects, micro-cracks etc [1]. In the supersaturated material, the hydrogen even causes formation of microscopic and mesoscopic defects, e.g. dislocations, cracks and "flakes" [51]. These effects may be the reason for the **hydrogen desorption**, observed upon pickling for prolonged time (> 200 sec). Obviously the formation of such defects allows formation of molecular hydrogen, which is leaving the material. This phenomenon is similar to the denitrogenation, observed after prolonged nitriding in NH$_3$ after formation of porosity and coalescence of pores to channels (see above). In practice, before continuous annealing the pickling times are in the range 19–22 s (HCl) in the case of the Al-killed steel and in the case of DP 600 between 5 s and 9 s, so that hydrogen effusion plays no role. But as mentioned before, during the subsequent annealing most hydrogen is desorbed and equilibrium with the N$_2$-H$_2$ atmosphere is established.

a)

b)
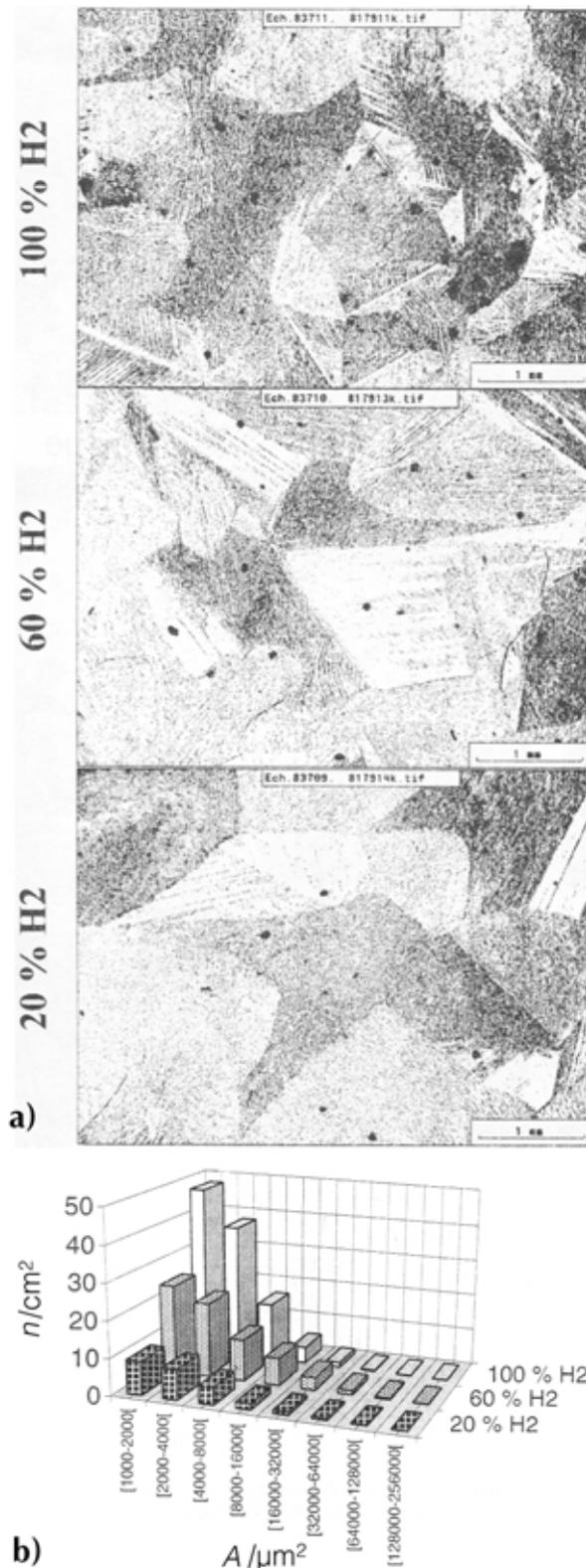
Figure 8: Blistering caused by hydrogen on a hot rolled low carbon steel after coating in a Zn-0.21 % Al-0.05 % Pb bath [38]; (a) tow views, black spots are blisters, (b) number n and size of blisters – at different H_2-contents of the annealing atmosphere

Slika 8: Mehurčkanje, povzročeno z navodičenjem pri vročem valjanju nizkoogljičnih jekel po cinkanju v Zn – 0,21 % Al – 0,05 % Pb -kopeli [38]

But enough hydrogen stays in the steel to cause some blistering of the zinc coating [37,38], see **Figure 8**.

4 SUPERSATURATION AND METAL DUSTING IN THE SYSTEM Fe-C

In contrast to both the systems discussed before, in which the nonmetal elements are gases, in this system the stable elemental form of the solute element is a solid, graphite, and the dissolution reaction:

$$C \text{ (graphite)} = [C] \qquad (10)$$

The most important carbide in the system Fe-C is cementite Fe_3C. About 50 years ago it was clearly shown by Darken and Gurry [52,53] that Fe_3C is metastable at all temperatures with respect to graphite and its saturated solution in iron. They established the famous Fe-C diagram, with the stable system Fe-graphite and the metastable $Fe-Fe_3C$ system, caring that the boundary lines were consistent with measured properties of the phases involved and the laws of thermodynamics. This phase diagram was later on repeatedly revised [54] but all subsequent diagrams have added only refinements in detail.

Here especially the data for formation of Fe_3C are of interest, the solubility of graphite c_C (gr) and solubility of cementite c_C (cem) in α-iron, and the carbon activity needed for cementite formation

$$a_C = c_C \text{ (cem)}/c_C \text{ (gr)}$$

The data in **Table 3** were presented by J. Chipman [54] in his review of the thermodynamics and phase diagram of the system Fe-C in 1972. It must be noted that there are different data for c_C (cem) in the literature, and obviously the solubility of Fe_3C in α-Fe can be enhanced, if its precipitates are formed under stress [55]. For stress-free cementite the solubility is lower.

Table 3: Solubility of graphite and cementite in α-Fe [52], carbon activity of cementite formation
Tabela 3: Topnost grafita in cementita v α-Fe [52], aktivnost ogljika pri tvorbi cementita

T/°C	µg/g graphite	µg/g cementite	a_C (Fe/Fe₃C)
300	0.013	0.21	16.2
350	0.081	0.75	9.3
400	0.37	2.3	6.2
450	1.35	5.7	4.2
500	4.3	13	3.0
550	11.7	28	2.39
600	28	57	2.04
650	63	102	1.62
700	127	160	1.26
727		218	
738	206		

But anyway, enhanced carbon activities $a_C > 1$ are necessary for cementite formation from α-iron

$$3\ Fe\ (\alpha) + C = Fe_3C \qquad (11)$$

The carbon may stem from a supersaturated solution or directly from an atmosphere with $a_C < 1$.

In ferrous metallurgy, the most well-known way to obtain cementite is by cooling or quenching out of the austenitic region. Depending on C content, cooling rate, holding times at different temperatures and alloying elements various structures are obtained: pearlite, bainite, tempered martensite which are basically assemblages of matrix and cementite in different microstructures.

Massive cementite can be prepared by reaction of carbon with iron powder alloyed with small contents of Cr or Mn, since these elements stabilize cementite, in this way by pressing and sintering samples were attained for determination of physical properties [56]. In the recent years, the formation of cementite by reaction with carburizing gas mixtures has gained wide interest, for two reasons:

1. To produce iron carbide in a direct reduction process from iron ore fines in natural gas (methane) at 600–650 °C under fluidized bed conditions. In contrast to sponge iron, which easily reoxidizes or even ignites [57], this "Iron Carbide Process" would produce non-reactive Fe_3C, for the use in electric arc furnaces [58-61].

2. Fe_3C is an intermediate on the corrosion process "metal dusting" which endangers steels in carburizing atmospheres (synthesis gas, reduction gas, hydrocarbons ...) in a temperature range 400–800 °C [62-67].

In the "Iron Carbide Process" the iron ores are reduced at first to iron sponge, which is to be converted to carbide by carburization according to

$$CH_4 + 3Fe = 2H_2 + Fe_3C \quad a_C = K_{12}\ \frac{p_{CH_4}}{p_{H_2}} \qquad (12)$$
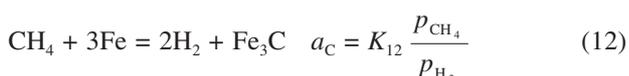
The latter reaction in fact takes place in the temperature range 400–800 °C [60,61,67-70] in spite of leading to an instable reaction product. Actually, the cementite produced from iron ore reduction and carburisation by CH_4-H_2 decomposes into iron and graphite, in both, the carburizing atmosphere and in an inert atmosphere (Ar gas). The rate of cementite decomposition increases up to 600 °C, where the rate is faster than at 700 °C [61], probably due to another morphology of the reaction products and control by C-diffusion in the iron (see below). That the "Iron Carbide Process" was no industrial success, most probably is rather caused by a strong retardation caused by the water vapour which stems from the reduction step. Already G. Simkovich and coworkers [68] had prepared Fe_3C from iron powder by the above reaction and studied its growth rate for determination of carbon diffusivity, but simultaneous decomposition will have occurred. A more reliable approach was taken by A. Schneider [69,70] who studied cementite formation in CH_4-H_2-H_2S, i.e. gas mixtures with a small addition of

H_2S which largely suppresses the cementite decomposition (see below).

The corrosion process "metal dusting" was studied, mainly in CO-H_2-H_2O mixtures, to simulate the attack of steels in synthesis or reduction gas, which is obtained by methane conversion. The mechanism of this process was elucidated for the reaction on iron and on low alloy steels, [62-67,71-74]. A description of the mechanism and its schematics was given before [2]. Carbon transfer occurs mainly by the reaction

$$CO + H_2 = H_2O + [C] \quad a_C = K_{13}\ \frac{p_{CO} \cdot p_{H_2}}{p_{H_2O}} \qquad (13)$$

The Boudouard-reaction

$$2\ CO = CO_2 + [C] \quad a_C = K_{14}\ \frac{p_{CO}^2}{p_{CO_2}} \qquad (14)$$
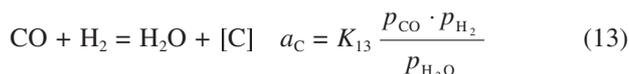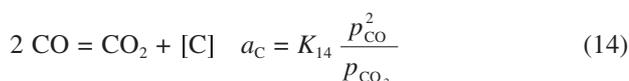
is much slower and does not play an important role in the kinetics and non-equilibrium thermodynamics of metal dusting. The surface reaction kinetics of reaction (13) is very fast and causes a rapid supersaturation of the surface-near region of an iron sample exposed to $CO + H_2$. The carbon diffuses inward and at the surface where the carbon activity is highest, Fe_3C nucleates. A nonuniform Fe_3C layer grows by carbon supply from the interior, the solid solution in α-iron, and by carbon transfer from the atmosphere to the Fe_3C surface.

Since C-diffusion in Fe_3C is rather slow compared to its diffusion in α-iron [68-70], the cementite particles in the surface are a barrier for the ingress of carbon, high carbon activities may be established on their surface and graphite can nucleate. This renders the Fe_3C instable (at $a_C = 1$) and its decomposition starts, in fact by inward growth of graphite as demonstrated by TEM-studies [71-74]. The C-atoms from the cementite attach to graphite planes, growing more or less vertically into the cementite. Intercalation of Fe-atoms between the graphite planes is possible and it was shown that iron is present in the graphite, diffuses outward, where the Fe-atoms coalesce to form particles of an average size of 20 nm. Such particles are catalytically very active and cause the "coke"-formation, **Figure 9**. The carbon is transferred by reaction (13) into the iron particles, and then nucleation and growth of graphitic carbon often leads to growth of carbon filaments from the particles, see **Figure 9c**.

In this way the reaction sequence results, which is typical for iron and low alloy steels and leads from a state of carbon in the atmosphere at a high a_C to the stable reaction products:

α-iron and graphitic carbon. After transfer of C from the atmosphere to states at

$$a_C > a_C\ (Fe/Fe_3C)$$

in the supersaturated solution in iron or in and on the cementite, the cementite decomposes according to
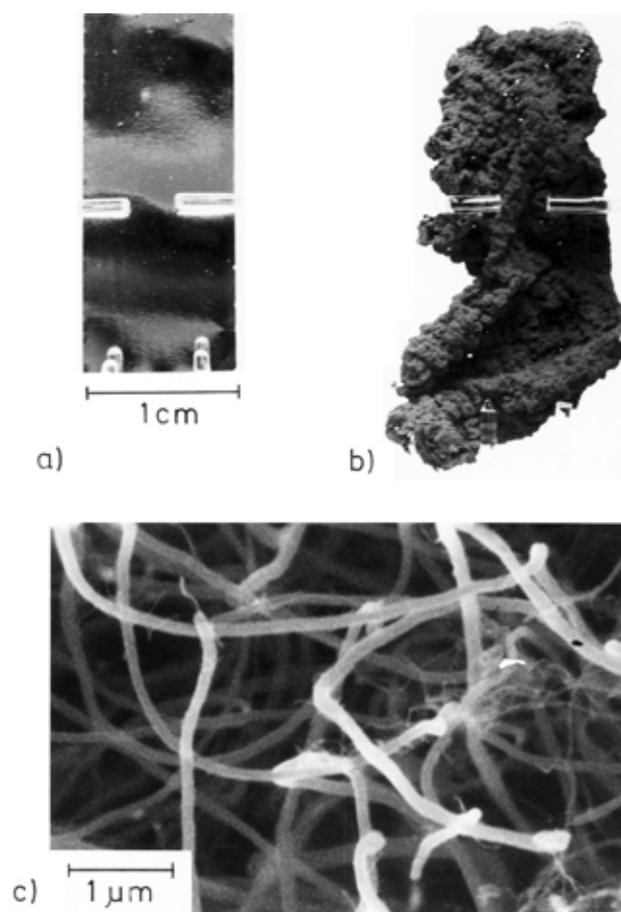
Figure 9: Metal dusting and formation of the reaction product "coke", i.e. a mixture of graphitic carbon and iron particles, on iron a) and b) iron sample before and after metal dusting attack in a CO-H_2-H_2O atmosphere and c) scanning electron micrograph of coke, showing the carbon filaments with metal particles at their end

Slika 9: Kovinsko prašenje (metal dusting) in tvorba reakcijskih produktov "koksa" (coke), mešanice grafita, ogljika in delčkov železa na železu a) in b) vzorec železa pred kovinskem prašenju in po njem v atmosferi CO-H_2-H_2O in c) SEM-posnetek "koksa" ki kaže ogljikova vlakna v kovinskih delcih

$$Fe_3C \rightarrow 3Fe(\alpha) + C \text{ (graphitic)} \qquad (15)$$
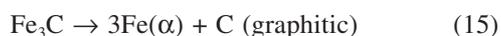
Under some conditions obviously the iron particles in the coke react back to cementite, maybe because they are exposed to the strongly carburizing atmosphere – at least cementite has been observed in the coke in several investigations [75-77]. But also cracking and spalling of cementite, due to growth stresses in the Fe_3C layer may cause transfer of metastable carbide into the reaction product "coke". The latter can have different morphologies [78,79] but generally is a black, magnetic, rather hard and porous composite of entangled carbon filaments and metallic particles. The kinetics of Fe_3C decomposition and coke growth on iron and low alloy steels, concerning dependences on time, partial pressures and temperature, have been studied in detail and are described elsewhere [63,65,67]. It may be noted that the time dependence of Fe_3C decomposition is linear, whereas the amount of coke
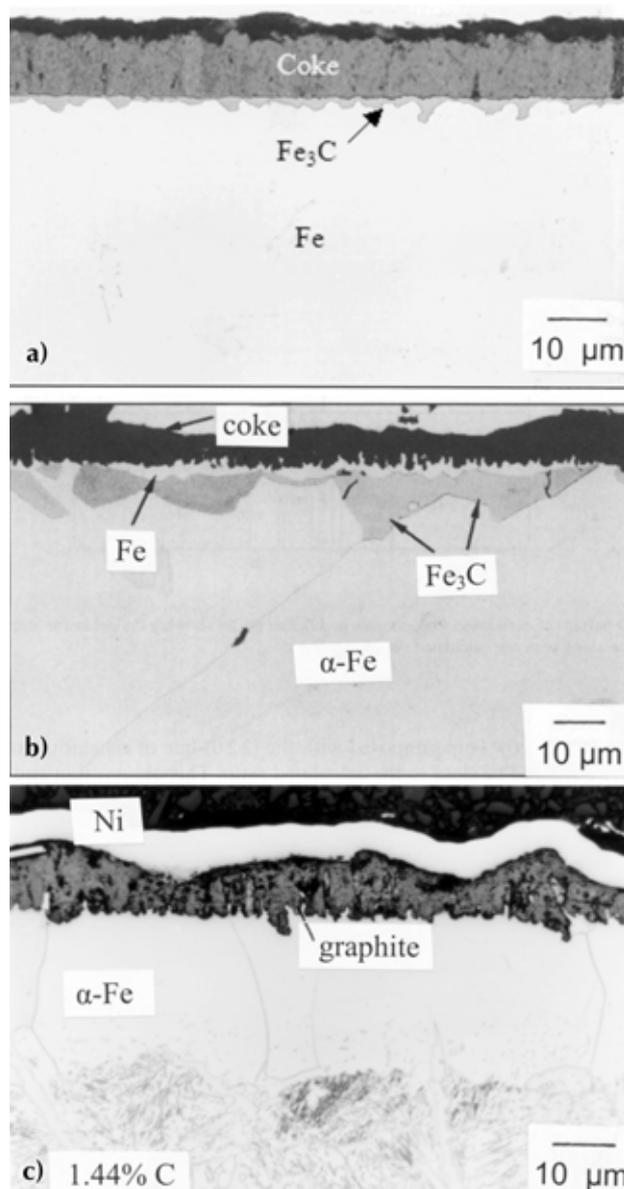
Figure 10: Graphite growth on supersaturated iron, of different origins and morphologies, shown by optical micrographs of metallographic cross sections of iron samples; (a) after 4 h in H_2-30 % CO-0.2 % H_2O at 600 °C, typical for steady state of metal dusting, (b) after 4 hours in H_2-5 % CO-0.2 % H_2O at 700 °C, showing inward growth of cementite and its outward decomposition under iron layer formation, the carbon diffuses through this layer so that graphite grows into the layer, (c) in corresponding state, but after carburization of iron in CH_4-H_2 at 1000 °C, then cooling and holding at 700 °C, the cementite formed in the supersaturated interior (1.44 % C) decomposes under formation of an inner Fe-layer and an outer graphite layer

Slika 10: Rast grafita na prenasičenem železu, različnega izvora in morfologije, prikazan s svetlobno mikroskopijo na metalografskih prerezih vzorcev železa a) po 4 h v H_2-30 % CO-0,2 % H_2O pri 600 °C, tipično za stabilno stanje kovinskega prašenja b) po 4 h v H_2-5 % CO-0,2 % H_2O pri 700 °C, prikazuje notranjo rast cementita in zunanji razpad pod nastalo plastjo železa, ogljik difundira skozi plast, tako da grafit raste v to plast c) v odgovarjajočem stanju, toda po naogljičenju železa v CH_4-H_2 pri 1000 °C, nato ohlajevanju in držanju pri 700 °C, tvorba cementita v prenasičenem okolju (1.44 % C) razkroj in tvorba notranje Fe-plasti ter zunanje grafitne plasti.

increases quadratically with time, due to the catalytic effect of the fine metal particles from Fe$_3$C decomposition. The typical morphology of metal dusting on iron is shown in **Figure 10a**: an outer layer of coke on the inner, irregular cementite layer which upon continued metal dusting approaches a steady state thickness of 0.5–1 μm [63].

With decreasing p_{CO} and increasing reaction temperature there is a tendency for formation of iron particles or even an iron layer on the cementite [80,81]. Obviously the probability increases, that the iron atoms from the Fe$_3$C decomposition can form bigger assemblages and eventually sinter to a continuous layer, see **Figure 10b**. Then the cementite decomposition will be limited by the outward diffusion of C through this layer, and its rate is effectively retarded. A corresponding decrease of attack by metal dusting on iron was observed at temperatures at 600–700 °C. That outward diffusion of C is rate limiting in this case, as can be seen from the morphology of the coke since the growth of inward protrusions of coke is favored by the shorter diffusion ways.

A corresponding morphology is observed also, if a supersaturated Fe-C sample or carbon steel are annealed at temperatures below 738 °C: cementite in the interior (pearlite structure), decarburized zone beneath the surface and a graphitic carbon layer on the surface. The cementite decomposes due to its instability, the carbon diffuses outward, and graphite grows on the surface with protrusions into the α-iron, they are growing faster because the diffusion way is shorter for their growth, see **Figure 10c**. The formation of graphitic deposits on carbon steels can occur in batch annealing, and may be harmful, causing bad adherence of tin or zinc coatings. Graphitization can be suppressed by the presence of sulfur and related elements, which inhibit the nucleation of graphite.

Finally the effect of sulfur on metal dusting [66,69,70] shall be explained. Presence of H$_2$S or other S-bearing compounds, such as CS$_2$, (CH$_3$)$_2$S$_2$ etc. in the atmosphere can retard or even suppress metal dusting, because sulfur is adsorbed strongly on metallic surfaces and also on Fe$_3$C [82,83], according to

H$_2$S = H$_2$ + S (adsorbed)
$$a_S = K_{16} \, p_{H_2S}/p_{H_2} \tag{16}$$

Already at low sulfur activities, a monolayer of adsorbed S is established on iron surfaces, which retards the carbon transfer from the atmosphere according to reactions (12), (13) and (14), and even more important, adsorbed sulfur hinders the nucleation of graphite. Therefore the decomposition of Fe$_3$C, reaction (15) is largely suppressed, and on iron and low alloy steels a slow growth of Fe$_3$C can continue for long time (e.g. at 600 °C if $p_{H_2S}/p_{H_2} \approx 10^{-6}$). This positive effect of sulfur has probably provided protection of steels in many plants, especially in refineries, where in the recent years in some cases [84,85] a decrease in sulfur content of the feedstock and/or an increase of operation temperature have caused failures, since at increased temperature, higher S additions are needed. Sulfur is also fine for protection of high alloy steels, which generally can be protected by oxide scales, i.e. spinel/chromia layers. But when such scale fails by cracking or spalling due to creep or thermal cycling, the sulfur can come in and seal the defects until they heal by a new oxide growth. Therefore in some plants, e.g. in heaters of direct reduction plants a high enough level of sulfur is maintained by dosing CS$_2$ or (CH$_3$)$_2$S$_2$. So in contrast to the system Fe-H where adsorbed sulfur promotes H-absorption into iron and steels, sulfur has a distinctly useful effect in the system Fe-C in suppressing a dangerous corrosion reaction.

5 CONCLUSIONS

The solid solubilities of the elements N, H and C in α-Fe are rather low in equilibrium with their thermodynamically stable states: N$_2$ (gas, 1 bar), H$_2$ (gas, 1 bar) and graphite, the solubilities in γ-Fe or iron melt are generally higher. So, supersaturated systems are obtained upon quenching after equilibration at higher temperatures.

Very high **supersaturation with nitrogen** and formation of the **instable nitrides** result from nitrogenation resp. nitriding in flowing NH$_3$-H$_2$ mixtures. Depending on the nitriding potential pNH$_3$/pH$_2$$^{3/2}$, nitrogen activities are obtained on the solid surface, which correspond to high nitrogen pressures and lead to formation of supersaturated Fe and of the γ'-, ε- and ζ-nitrides. In fact, no equilibrium is established but a **steady state**, resulting from the reaction NH$_3$ = [N] + 3/2 H$_2$ which is fast already at temperatures > 300 °C, and the nitrogen desorption 2 [N] → N$_2$ which becomes notable only at high temperatures > 700 °C. Furthermore, at the iron surface the latter reaction is easily suppressed by adsorbed oxygen, sulfur and other surface impurities. But due to the high virtual nitrogen pressures within the supersaturated phases, N$_2$-formation can occur in nitrided or carbonitrided iron and steels causing **porosity**. Later, coalescence of voids and channel formation may lead to **denitrogenation**.

Supersaturation with hydrogen can have very serious consequences for iron and steels, either by occurrence of **voids and pores** in the material and **blisters** below coatings, caused by formation of **molecular hydrogen** at high pressure; or by the action of rapidly diffusing **atomic hydrogen** in crack initiation and propagation, i.e. **hydrogen embrittlement**. As mentioned, supersaturation is possible by quenching, after annealing in H$_2$ containing atmospheres at elevated temperatures, but generally the H$_2$ desorption is fast, if not impeded by coatings. Another important way of supersaturation with hydrogen is by **acid corrosion,** e.g.

upon pickling of steels. By the interplay of the dissolution reaction $Fe = Fe^{2+} + 2e^-$ and hydrogen discharge $2H^+ + 2e^- = 2 H(ad) = H_2$, in this process a **steady state** is attained for the electrochemical potential and the surface concentration of adsorbed H. Again surface impurities such as sulfur etc. inhibit the recombination reaction, increase the surface concentration of H(ad) and "promote" hydrogen absorption in steels. The high hydrogen contents absorbed can cause formation of dislocations and microcracks, leading to **hydrogen loss** after continued pickling.

Supersaturation with carbon and **formation of the instable carbide cementite** Fe_3C occurs in nonequilibrium atmospheres: CH_4-H_2, CO-H_2-H_2O, CO-CO_2 and hydrocarbons at carbon activities $a_C > 1$. The **cementite formation** is wanted in the "**iron carbide process**" for production of cementite by direct reduction of iron ores, but it is fatal in process industries and direct reduction plants, where such atmospheres cause "**metal dusting**" of steel components. Cementite decomposes into iron and graphite, at a rate which is increasing up to about 600 °C. A dust of graphitic carbon and fine metal particles results from **cementite decomposition** and the metal particles are catalysts for additional carbon deposition, mostly as filamentous carbon. In the normal case of metal dusting an irregular front of cementite progresses into the supersaturated metal phase, followed by graphite growing into the cementite, which is covered by the "coke", generally composed of carbon filaments and fine metal particles. This **steady state process** leads to linear kinetics for metal consumption and a quadratic increase of coke with time. Since at higher temperatures, an iron layer may be formed between the graphitic carbon on the surface and the decomposing cementite, this decomposition becomes controlled by carbon diffusion in the iron layer and is retarded. A similar morphology is observed upon batch annealing of carbon steels when the cementite in the interior decomposes and graphite segregates on the steel surface. Presence of adsorbed sulfur can suppress graphite nucleation and cementite decomposition in these processes of graphitization and metal dusting and thus **sulfur and related elements stabilize cementite**.

Acknowledgement

6 REFERENCES

[1] H. J. Grabke, E. Riecke: Mater. Tehnol. 34 (**2000**), 331

[2] H. J. Grabke: Mater. Tehnol. 36 (**2002**), 297

[3] J. D. Fast: Interaction of Metal and Gases, Academic Press 1965

[4] V. G. Paranjpe, M. Cohen, M. B. Bever, C. F. Floe: Trans AIME 188 (**1959**), 261

[5] I. Aydin, H. E. Bühler, A. Rahmel: Werkstoffe & Korrosion 31 (**1980**), 675

[6] E. Lehrer: Z. Elektrochem. 36 (**1930**), 383 and 460

[7] "Nitrieren und Nitrocarburieren" Ed. E. J. Mittemeijer, J. Grosch, Berichtsband AWT Tagung April 1991, Darmstadt

[8] "Nitrieren und Nitrocarburieren" Ed. J. Grosch, E. J. Mittemeijer, Berichtsband AWT Tagung April 1996, Weimar

[9] H. J. Grabke: Berichte Bunsenges. physikal. Chemie 72 (**1968**), 533 and 548

[10] Itaru Niimi, Akihiko Satomi: 8th Heat Treating Conference, American Soc. for Metals, Sept. 1984

[11] E. J. Mittemeijer, M. van Rooyen, I. Wierszyllowski, H.C.F. Rozendaal, P. F. Colijn: Z. Metallkde 74 (**1983**), 473

[12] H. J. Grabke: Arch. Eisenhüttenwes. 44 (**1973**), 603

[13] H. J. Grabke, E. M. Petersen, S. R. Srinivasan; Surface Sci 67 (**1977**), 501

[14] H. J. Grabke: Materials Sci. Eng. 42 (**1980**), 91

[15] H. J. Grabke: Berichte Bunsenges. physikal. Chemie 73 (**1969**), 596–601

[16] M. A. J. Somers, N. M. van der Pers, D. Schalkoord, E. J. Mittemeijer: Metallurg. Trans 20A (**1989**), 1533

[17] M. A. J. Somers, E. J. Mittemeijer: Metallurg. Mat. Trans 26A (**1995**), 57

[18] E. J. Mittemeijer, M. A. J. Somers: Surface Engineering 13 (**1997**), 483

[19] B. J. Kooi, M. A. J. Somers, E. J. Mittemeijer: Metallurg. Mat. Trans. 25A (**1994**), 2797

[20] F. Hoffmann, H. Kunst, H. Klümper-Westkamp, D. Liedtke, E. J. Mittemeijer, E. Rose, K. Zimmermann: "Stand der Kenntnisse über die Porenentstehung beim Nitrieren und Nitrocarburieren" in ref. 7, 105–113

[21] D. Liedtke: "Bedeutung poröser Verbindungsschichten für die technische Anwendung", in ref. 7, 114–121

[22] R. Hoffmann: "Stand der Vorstellungen zur Porenbildung", in ref. 8, 29–42

[23] D. L. Williamson, O. Ozturk, R. Wei, P. J. Wilbur: Surf. Coatings Technol. 65 (**1994**), 15

[24] O. Ozturk, D. L. Williamson: J. Appl. Phys. 77 (**1995**), 3839

[25] K. Gemma, Y. Satoh, I. Ushioku, M. Kawakami: Surf. Eng. 11 (**1995**), 240

[26] H. J. Grabke: Materials & Corrosion in press

[27] Y. Cao, F. Ernst, G. M. Michal: Acta Mat. S1 (**2003**), 4171

[28] R. A. Oriani: Acta Met. 18 (**1979**), 147

[29] E. Riecke: Arch. Eisenhüttenwes. 44 (**1973**), 647–656

[30] E. Riecke: Werkst. Korros. 29 (**1978**), 106–112

[31] E. Riecke: 8th Intern. Congress on Metallic Corrosion, Main 1 (1981) 605–610

[32] J. P. Hirth: Metallurg. Trans 11A (**1980**), 861

[33] P. Neumann: Stahl u. Eisen 107 (**1987**), 577

[34] W. Haumann; W. Heller, H. A. Jungblut, H. Pircher, R. Pöpperling, W. Schwenk: Stahl u. Eisen 107 (**1987**), 585

[35] Hydrogen Transport and Cracking in Metals, Turnbull, E. [ed.:] The Inst. of Materials, London 1995

[36] H. J. Grabke, F. Gehrmann, E. Riecke: Steel Research 72 (**2001**), 225

[37] Th. Schlüter: "Wasserstoffaufnahme während des Beizens und des Glühens von warmgewalztem Stahlband vor der Feuerverzinkung" Dr-thesis, Universität Dortmund Fachbereich Chemie, April 1991

[38] L. Bordignon, D. LeJeune, B. Schumacher, M. Meurer, K. Uran, H.J. Grabke, T. Schlüter: "Galvanising of hot-rolled steel strip" ECSC report EUR 20345 EN, Europ. Comm. 2002

[39] H. Kaesche: Die Korrosion der Metalle, Springer, Heidelberg, 1979

[40] R. Pöpperling, W. Schwenk: Werkst. u. Korros. 31 (**1980**), 15

[41] M. A. V. Devanathan, Z. Stachurski: Proc. Roy. Soc. A 270 (**1962**), 90

[42] M. A. V. Devanathan, Z. Stachurski: J. electrochem. Soc. 111 (**1964**), 619

[43] E. Riecke, B. Johnen, H. J. Grabke: Werkst. Korros. 36 (**1985**), 435

[44] E. Riecke, R. Möller, B. Johnen, H. J. Grabke: Werkst. Korros. 36 (**1985**), 447

[45] E. Riecke, B. Johnen, H. J. Grabke: Werkst. Korros. 36 (**1985**), 455

[46] E. Riecke, R. Möller, B. Johnen: Corros. Sci. 27 (**1987**), 1027

[47] E. Riecke, H. Liesegang, H. J. Grabke: Werkst. Korros. 38 (**1987**), 310

[48] E. Riecke, B. Johnen, H. Liesegang, A. Thoms, B. Reynders, H. J. Grabke: Werkst. Korros. 39 (**1988**), 525

[49] E. Riecke, B. Johnen: Werkst. Korros. 42 (**1991**), 528

[50] E. Riecke, B. Johnen: Werkst. Korros. 42 (**1991**), 626

[51] S. D. Kapusta, T. T. Kam, K. E. Heusler: Z. phys. Chemie N.F. 123 (**1980**), 219

[52] L. S. Darken, R. W. Gurry: AIME Trans. (**1951**), 1015

[53] L. S. Darken, R. W. Gurry: The Physical Chemistry of Metals McGraw-Hill, New York 1953

[54] J. Chipman: Met. Trans. 3 (**1972**), 55

[55] J. C. Swartz: Trans. Met. Soc. AIME 245 (**1969**), 1083

[56] W. Jellinghaus: Archiv Eisenhüttenwes. 37 (**1966**), 181

[57] H. J. Grabke, R. Steffen, A. Jess, D. Steyls: "Reoxidation and ignition behaviour of direct reduced iron" ECSC final report, EUR 20632 EN, Brussels 2003

[58] G. H. Geiger, F. A. Stephens: "Steelmaking with Iron Carbide" Ironmaking conference proceedings ISS-AIME 52 (1993) Dallas Tx

[59] L. Kolbeinsen, T. Båsen: "Ferrocarbon-Production and Use of Iron Carbide" in Metallurg. Processes for Early Twenty-first Century. Ed. H. Y. Sohn TMMMS 1994

[60] R. H. Gronebaum, W. Pluschkell: "Investigations on the Iron Carbide Formation Reaction", Int. Conf. "Prereduced Products and Europe" Milano Sept. 1996 Assoc. Italiana de Metallurgia

[61] J. Zhang, O. Ostrowski: ISIJ Int. 41 (**2001**), 333, 340

[62] H. J. Grabke, R. Krajak, J. C. Nava Paz: Corrosion Sci. 35 (**1993**), 1141–1150

[63] H. J. Grabke, C. B. Bracho Troconis, E. M. Müller-Lorenz: Werkst. u. Korr. 45 (**1994**), 215–221

[64] H. J. Grabke: Corrosion NACE 51 (**1995**), 711–720

[65] H. J. Grabke: Mat. Corr. 49 (**1998**), 303–308

[66] H. J. Grabke, E. M. Müller-Lorenz, A. Schneider: ISIJ International 41 (**2001**), Supplement S1-S8

[67] H. J. Grabke: Mat. & Corr. 54 (**2003**), 736

[68] B. Ozturk, V. L. Fearing, J. A. Ruth, G. Simkovich: Met. Trans 13A (19832) 1871, Solid State Ionics 12 (**1984**), 145

[69] A. Schneider, G. Inden, H. J. Grabke, Q. Wei, E. Pippel, J. Woltersdorf: steel research 71 (**2000**), 179/84

[70] A. Schneider, H. J. Grabke: Mat. & Corr. 54 (**2003**), 793

[71] E. Pippel, J. Woltersdorf, H. J. Grabke, S. Strauß: steel research 66 (**1995**), 217–221

[72] Q. Wei, E. Pippel, J. Woltersdorf, H. J. Grabke: Mat. & Corr. 50 (**1999**), 628–633

[73] C. M. Chun, T. A. Ramanarayanan, J. D. Mumford: Mat. & Corr. 50 (**1999**), 634

[74] C. M. Chun, J. D. Mumford, T. A. Ramanarayanan: J. Electrochem. Soc. 149 (**2002**), B 348

[75] Z. Zeng, K.Natesan, V. A. Maroni; Oxid. Met. 58 (**2002**), 147

[76] J. Zhang, A. Schneider, G. Inden: Corros. Sci. 45 (**2003**), 281, 1329

[77] C. H. Toh, P. R. Munroe, D. J. Young: Oxid. Met. 58 (**2002**), 1

[78] E. M. Müller-Lorenz, H. J. Grabke: Mat. Corr. 50 (**1999**), 614–621

[79] J. Zhang, A. Schneider, G. Inden: Mat. & Corr. 54 (**2003**), 770

[80] A. Schneider: Corros. Sci. 44 (**2002**), 2353

[81] J. Zhang, A. Schneider, G. Inden: Mat. & Corr. 54 (**2003**), 763

[82] A. Schneider, H. Viefhaus, G. Inden: Mat. & Corr. 51 (**2000**), 338

[83] H. J. Grabke, D. Moszynski, E. M. Müller-Lorenz, A. Schneider: Surface Interface Analysis 34 (**2002**), 369

[84] M. H. Ravestein: Corrosion '97, NACE Houston Texas 1997, paper No. 496

[85] H. J. Grabke, M. Spiegel; Mat. & Corr. 54 (**2003**), 299